

Pomeron loops in zero transverse dimensions

Arif I. Shoshi^{1, 2,*} and Bo-Wen Xiao^{1, †}

¹*Department of Physics, Columbia University, New York, NY, 10027, USA*

²*Fakultät für Physik, Universität Bielefeld, D-33501 Bielefeld, Germany*

(Dated: May 24, 2019)

We analyze a toy model which has a structure similar to that of the recently found QCD evolution equations, but without transverse dimensions. We develop two different but equivalent methods in order to compute the leading-order and next-to-leading order Pomeron loop diagrams. In addition to the leading-order result which has been derived from Mueller’s toy model [1], we can also calculate the next-to-leading order contribution which provides the $(\alpha_s^2 \alpha Y)$ correction. We interpret this result and discuss its possible implications for the four-dimensional QCD evolution.

PACS numbers: 12.38.Cy; 11.10.Hi; 11.55.Bq

I. INTRODUCTION

There have been major breakthroughs in understanding high-density QCD evolution recently. Several important observations have been made: (i) gluon number fluctuations have a big effect on the evolution towards gluon saturation [2], (ii) a connection between high-energy QCD evolution and statistical physics models of reaction-diffusion type was found [3, 4] which has clarified the interpretation of fluctuations in an event-by-event picture, and (iii) it was realized that the relevant fluctuations are missed [5] by the existing Balitsky-JIMWLK equations [6, 7]. These observations have led to the creation of new QCD evolution equations which include gluon number fluctuations or Pomeron loops [8, 9, 10, 11].

The new equations describe the usual BFKL evolution, Pomeron splittings and Pomeron mergings and, thus, through iterations, Pomeron loops. A lot is known about the structure of the new equations [12, 13, 14, 15, 16], however, because of their complexity, little about their solutions. So far, analytical results for the energy dependence of the saturation momentum and for the scaling behavior of the T -matrix at asymptotic energies [2, 5] and some numerical simulations of approximations to the exact equations [16, 17] are available. Solutions to the new equations in the range of collider energies are desired.

In this paper, we consider a toy model which has a structure similar to that of the new QCD evolution equations, but which has no transverse dimensions. This simplification allows an exact solution of the evolution equations. The particle-particle scattering amplitude is calculated. The effects of saturation and unitarity, or “Pomeron” loops which are the characteristics of the new evolution equations, are investigated.

A decade ago, Mueller [1] studied a similar toy model without transverse dimensions which was motivated by the QCD dipole model [18]. He has been able to solve the toy model exactly and calculate the S -matrix. Ob-

servations made by studying this toy model (e.g. the one that fluctuations in particle numbers lead to a divergent multiple scattering series) have been shown numerically [19, 20] to be valid also in the four-dimensional QCD. The hope that some of the results obtained in the toy model discussed in this paper may also apply in four-dimensional QCD is one of the motivations for this work.

In the toy model proposed by Mueller [1], particle-particle scattering in the center-of-mass frame at total rapidity Y was considered. In this model, each particle evolves to a dense system through particle branching (splitting). Unitarity effects (at leading order accuracy) are correctly described due to the multiple scatterings between the dense systems. There are no particle mergings in the wavefunctions of the particles in this model, therefore, the model fails to describe saturation effects in the wavefunctions of the particles which become important at very high rapidities. In the language of loops, only the loops stretching over the rapidity interval greater than $Y/2$ (“large” loops) shown e.g. in Fig. 1B are included (at leading-order accuracy). “Large” loops are created by matching the evolution (“Pomeron” splittings) of both particle’s wavefunctions at $Y/2$. However, there are no loops inside the particle’s wavefunctions (“small” loops) where the “Pomeron” splits and merges, as shown e.g. in Fig. 1C, within the rapidity interval $Y/2$. The above limitations of the toy model are, of course, properties of the QCD dipole model [18] as well and are well-known.

Our toy model which is inspired by the new QCD evolution equations [8, 9, 10, 11] allows us to study unitarity effects as well as saturation effects. We calculate the leading order (LO) and the next-to-leading order (NLO) loop contributions to the particle-particle scattering amplitude. The LO result, which is the LO contribution of the “large” loops, agrees with the result from [1]. Our NLO result consisting of the NLO contribution of the “large” loops and the LO contribution of the “small” loops is new. The NLO correction with respect to the LO result is of order $\alpha_s^3 Y$. This is the main result of the paper. It tells us that the NLO contribution is negligible as compared with the LO contribution up to rapidities $Y \leq 1/\alpha_s^3$.

Presumably our toy model reveals the properties of the

*Electronic address: shoshi@physik.uni-bielefeld.de

†Electronic address: bowen@phys.columbia.edu

four-dimensional QCD evolution to some extent. In fact, its behavior is a heuristic sign that the NLO contribution can be neglected in the QCD evolution as well as long as $Y \ll 1/\alpha_s^3$. Such a NLO correction seems to appear also in real QCD. Taking the one-loop diagram for example, the LO contribution in QCD is $(\alpha_s^2)^2 \exp(2\alpha Y)$ which comes from varying the size of the loop from 0 to Y , where $\alpha = \alpha_P - 1 = \frac{4\alpha_s N_c}{\pi} \ln 2$. The NLO contribution $(\alpha_s^2)^2 \alpha Y \exp(\alpha Y)$ comes from changing the location of a fixed zero-size loop from 0 to Y . The suppression of the NLO contribution by the factor $\alpha Y/e^{\alpha Y}$ directly leads to the general correction $\alpha_s^2 \alpha Y$ (the same happens in our toy model).

Such a NLO correction $(\alpha_s^3 Y)$ in QCD was unexpected for the following reason: For dipole-dipole scattering in the center-of-mass frame, we know that unitarity effects become nonnegligible when the two-Pomeron exchange becomes of the order of the one-Pomeron exchange, which is the case when $Y_U \sim \frac{1}{\alpha_s} \ln \frac{1}{\alpha_s^2}$. (Equivalently, at Y_U “large” Pomeron loops become important since the correction brought in by the extra BFKL ladder, $\alpha_s^2 \exp(\alpha_s Y)$, is of order one.). Saturation effects (“small” Pomeron loops) are widely expected to become important at the same order of rapidity, $Y_s \sim 2Y_U$, in the center-of-mass frame (see, e.g. ref. [21]). Our toy model, however, is telling us that the NLO corrections become important at a parametrically much higher rapidity $Y \sim 1/\alpha_s^3$. If this is the case also in four-dimensional QCD, then Mueller’s LO Pomeron-loop result for dipole-dipole scattering [1] calculated within his QCD dipole model [18], i.e., the Borel-summed multiple-Pomeron series, is a good approximation until $Y \lesssim 1/\alpha_s^3$, instead of $Y \lesssim \frac{2}{\alpha_s} \ln \frac{1}{\alpha_s^2}$ as believed.

The paper is organized as follows: In Sec. II, we show the toy model. Two methods are developed in order to solve the toy model and some discussion is provided on the consequences of the NLO corrections. They are explained in Sec. III. In the Appendices we show the Lorentz-invariance of the toy model and give the solution to another commonly used zero-dimensional model. Finally, we discuss the results and give the conclusions.

II. A TOY MODEL WITH “POMERON” LOOPS

In this section, we consider a toy model without transverse dimensions which has a structure similar to that of the recently found four-dimensional QCD evolution equation [8, 9, 10, 11]. The toy model describes the rapidity evolution of the particle number n of a system. The dynamics in zero-transverse dimensions is given by

the following Langevin equation¹

$$\frac{d\tilde{n}}{dy} = \alpha\tilde{n} - \beta\tilde{n}^2 + \sqrt{2\alpha\tilde{n}} \nu(y) \quad (1)$$

where $\nu(y)$ is a Gaussian white noise: $\langle \nu(y) \rangle = 0$ and $\langle \nu(y)\nu(y') \rangle = \delta(y - y')$. Eq. (1) is known as the zero transverse dimensional “Reggeon field theory” equation and it contains the projectile-target duality (see Appendix A). The structure of Eq. (1) is obvious: the first term on the r.h.s. represents the growing of the particles, the second term describes particle recombinations which limit the growth at a maximum occupancy, and the third term describes the particle number fluctuations. These are essentially the main ingredients of the real QCD equations.

With Ito’s calculus, one can write Eq. (1) into an infinite hierarchy of coupled evolution equations,

$$\frac{dn^{(k)}}{dy} = k\alpha n^{(k)} + k(k-1)\alpha n^{(k-1)} - k\beta n^{(k+1)}, \quad (2)$$

where $n^{(k)} = \langle : \tilde{n}^k : \rangle$ is the expectation value of k -particles during the evolution and it should be understood as a normal ordered number operator (i.e. the factorial moment $\langle \tilde{n}(\tilde{n}-1)\cdots(\tilde{n}-k+1) \rangle$) according to its physical interpretation. Here, $k\alpha n^{(k)}$ is the growth term, $k(k-1)\alpha n^{(k-1)}$ the fluctuation term, and $k\beta n^{(k+1)}$ the recombination term. Eqs. (1, 2) are the zero-transverse-dimensional analog of the real QCD equations (see [5, 9]). A simple derivation and a discussion in the context of QCD evolution of eqs. (1, 2) can be found in [5]. The solution to another widely discussed Langevin equation is shown in Appendix B.

III. SOLUTION TO THE TOY MODEL

Eq. (2) is quite complicated since $n^{(k)}$ is coupled with $n^{(k-1)}$ and $n^{(k+1)}$ in the evolution, i.e., Eq. (2) is just a particular equation within an infinity hierarchy of coupled equations. However, the following observation helps to solve Eq. (2): the fixed point is $n^{(k)} = (\alpha/\beta)^{(k)}$ and the particle number at high Y saturates at $n_s = \alpha/\beta$. Since we like to have $n_s \gg 1$ in order to be close to the real QCD case, it follows that $\beta \ll \alpha$, which means that the recombination term can be neglected as compared to the growth and fluctuation terms in Eq. (2) until the unitarity limit is reached. Therefore, if one starts with a dilute object at $Y = 0$ ($n \ll n_s$), then one can consider the evolution equation without the recombination term at the early stages of the evolution, and turn on the recombination term as a perturbation at the end of

¹ We provide the solution to the zero transverse dimensional sFKPP equation with a different noise term $\sqrt{2(\alpha\tilde{n} - \beta\tilde{n}^2)} \nu(y)$ in Appendix. B

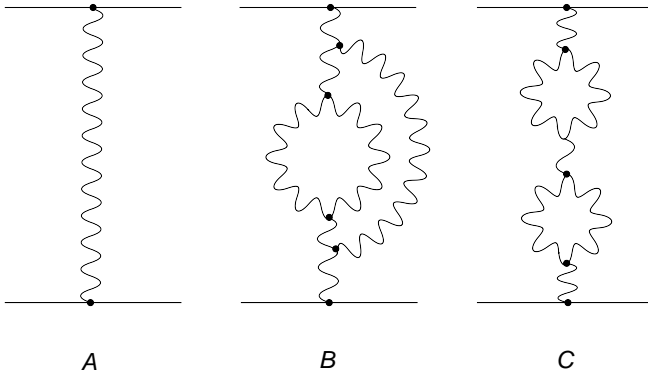


FIG. 1: Three kinds of reggeon graphs, in which the curly lines represent BFKL ladders. Diagram (A) is a simple BFKL ladder exchanged between the two particles (horizontal lines); Diagram (B) is the LO Pomeron loop diagram which has been calculated in ref. [1, 20, 22]; Diagram (C) is the NLO pomeron loop diagram which was not included in the dipolar approach of ref. [1, 20, 22] while it can be computed in this toy model.

the evolution which forms the “Pomeron” loops. Following this philosophy, we have found two different methods to solve Eq. (2) which we will present in the following subsections. Before entering the calculations, we should state that we always work in a parametrical limit in which $\alpha_s^2 \rightarrow 0$ and $\alpha Y \rightarrow \infty$, but $\alpha_s^2 e^{\alpha Y}$ is fixed and finite.

A. Method I: Integral Representation

Eq. (2) without the recombination term,

$$\frac{dn_0^{(k)}}{dy} = k\alpha n_0^{(k)} + k(k-1)\alpha n_0^{(k-1)}, \quad (3)$$

can be solved exactly if given some physically chosen initial conditions. In this paper, we consider the evolution of a single particle for which the initial conditions are $n_0^{(1)}|_{y=0} = N$ and $n_0^{(k)}|_{y=0} = 0$. The solution to Eq. (3) with the above initial conditions reads

$$n_0^{(k)}(y) = N k! e^{k\alpha y} (1 - e^{-\alpha y})^{k-1} \quad (4)$$

and corresponds to the k -particle density obtained via splitting from a single particle after the evolution over the rapidity y . To turn on the perturbation, let us start with the first equation in the infinite hierarchy (2),

$$\frac{dn_1^{(1)}}{dy} = \alpha n_1^{(1)} - \beta n_0^{(2)}, \quad (5)$$

which has the solution

$$\begin{aligned} n_1^{(1)}(Y) &= n_0^{(1)}(Y) - \beta \int_0^Y dy e^{\alpha(Y-y)} n_0^{(2)}(y) \\ &= N e^{\alpha Y} - 2 \frac{\beta}{\alpha} N e^{2\alpha Y} (1 - \frac{\alpha Y}{e^{\alpha Y}} - \frac{1}{e^{\alpha Y}}). \end{aligned} \quad (6)$$

It is straight forward to recognize that the first term in Eq. (6) is the usual BFKL term, and the second term corresponds to the one-loop diagram with the right intrinsic minus sign. One can also see that $\frac{\alpha Y}{e^{\alpha Y}}$ is the NLO contribution in the parametrical limit we mentioned above.

To get the LO two-loop diagram shown in Fig. 1 B, we start with the second equation in Eq. (2),

$$\frac{dn_1^{(2)}}{dy} = 2\alpha n_1^{(2)} + 2\alpha n_0^{(1)} - 2\beta n_0^{(3)}, \quad (7)$$

whose solution is

$$\begin{aligned} n_1^{(2)}(Y) &= n_0^{(2)}(Y) - 2\beta \int_0^Y dy e^{2\alpha(Y-y)} n_0^{(3)}(y) \\ &= 2N e^{2\alpha Y} (1 - e^{-\alpha Y}) - 2 \cdot 3! \frac{\beta}{\alpha} N e^{3\alpha Y} (1 - \frac{2\alpha Y}{e^{\alpha Y}} + \dots), \end{aligned} \quad (8)$$

then turn on the perturbation, $\frac{dn_2^{(1)}}{dy} = \alpha n_2^{(1)} - \beta n_1^{(2)}$, in order to take into account the recombination from $n^{(2)}$ to $n^{(1)}$ (in addition to the recombination from $n_0^{(3)}$ to $n^{(2)}$ given by Eq. (7)), which leads to

$$\begin{aligned} n_2^{(1)}(Y) &= n_0^{(1)}(Y) - \beta \int_0^Y dy e^{\alpha(Y-y)} n_1^{(2)}(y) \\ &= N e^{\alpha Y} - 2 \frac{\beta}{\alpha} N e^{2\alpha Y} (1 - \frac{\alpha Y}{e^{\alpha Y}} - \frac{1}{e^{\alpha Y}}) + 3! \left(\frac{\beta}{\alpha} \right)^2 N e^{3\alpha Y} (1 - \frac{4\alpha Y}{e^{\alpha Y}} + \mathcal{O}(\frac{1}{e^{\alpha Y}})). \end{aligned} \quad (9)$$

The third term in Eq. (9) represents the LO two-loop diagram shown in Fig. 1 B.

In order to calculate the NLO two-loop diagram shown in Fig. 1 C, one has to enforce a recombination to happen after a splitting. Thus, starting with $n_0^{(1)} = Ne^{\alpha Y}$, one splitting given by $n_2^{(0)}(Y) = 2\alpha \int_0^Y dy e^{2\alpha(Y-y)} n_0^{(1)}(y)$, followed by one merging $\Delta n_1^{(1)} = -\beta \int_0^Y dy e^{\alpha(Y-y)} n_0^{(2)}(y)$, yields the result for the one-loop diagram. A further splitting and a subsequent merging gives the result for the NLO two-loop diagram,

$$\Delta n^{(1)}(Y) = 3! \left(\frac{\beta}{\alpha} \right)^2 Ne^{3\alpha Y} \left(\frac{2}{3} \frac{\alpha Y}{e^{\alpha Y}} + \mathcal{O} \left(\frac{1}{e^{\alpha Y}} \right) \right) . \quad (10)$$

In fact, in order to calculate any loop diagram, one just needs to know the merging and splitting vertices which according to Eq. (2) read, respectively,

$$\Delta n_m^{(k)}(Y) = -k\beta \int_0^Y dy e^{k\alpha(Y-y)} \Delta n^{(k+1)}(y) , \quad (11)$$

$$\Delta n_s^{(k)}(Y) = k(k-1)\alpha \int_0^Y dy e^{k\alpha(Y-y)} \Delta n^{(k-1)}(y) . \quad (12)$$

For particle-particle scattering, the $(k+1)$ -th order diagram contains k -splittings and k -mergings: The leading-order diagram corresponds to the diagram in which all k -splittings occur before all the k -mergings, the next-to-leading order diagram is always the diagram in which exactly one merging takes place before one splitting. The sum over all LO and NLO loop diagrams gives the LO and NLO contributions to the T -matrix, respectively.

For particle-particle scattering, the sum over the LO loop diagrams (leading and next-to-leading contribution) reads

$$n_{LO}^{(1)}(Y) = \sum_{k=1}^{\infty} (-1)^{k+1} N \cdot k! e^{k\alpha Y} \left(\frac{\beta}{\alpha} \right)^{k-1} \left(1 - (k-1)^2 \frac{\alpha Y}{e^{\alpha Y}} + \mathcal{O} \left(\frac{1}{e^{\alpha Y}} \right) + \mathcal{O} \left(\left(\frac{\alpha Y}{e^{\alpha Y}} \right)^2 \right) \right) , \quad (13)$$

while the sum over the NLO loop diagrams (leading contribution) is

$$n_{NLO}^{(1)}(Y) = \sum_{k=1}^{\infty} (-1)^{k+1} N \cdot k! e^{k\alpha Y} \left(\frac{\beta}{\alpha} \right)^{k-1} \left(\frac{(k-1)(k-2)^2}{k} \frac{\alpha Y}{e^{\alpha Y}} + \mathcal{O} \left(\frac{1}{e^{\alpha Y}} \right) + \mathcal{O} \left(\left(\frac{\alpha Y}{e^{\alpha Y}} \right)^2 \right) \right) . \quad (14)$$

The resulting S -matrix, $S \equiv 1 - T$ (with $T = \alpha_s^2(n_{LO}^{(1)} + n_{NLO}^{(1)})$), which includes LO and NLO loop diagrams, can be written in the form

$$S(Y) = \sum_{k=0}^{\infty} (-1)^k \cdot k! (\alpha_s^2 e^{\alpha Y})^k \left\{ 1 + \alpha_s^2 \alpha Y \cdot (3k^2 - k) + \alpha_s^2 \cdot f_1(k) + (\alpha_s^2 \alpha Y)^2 \cdot f_2(k) + \dots \right\} , \quad (15)$$

where we have put $\frac{\beta}{\alpha} = \alpha_s^2$ in close analogy with the four-dimensional QCD and $N = 1$. $f_1(k)$ and $f_2(k)$ are functions of k , which are too complicated to be calculated in this method. The series in Eq. (15) is a divergent series, however, it is Borel-summable. After the Borel-summation, the expression for the S -matrix becomes rather complicated,

$$\begin{aligned} S(Y) &= \frac{1}{\alpha_s^2 e^{\alpha Y}} \exp \left(\frac{1}{\alpha_s^2 e^{\alpha Y}} \right) \Gamma \left(0, \frac{1}{\alpha_s^2 e^{\alpha Y}} \right) \\ &+ (\alpha_s^2 \alpha Y) \left\{ \frac{1}{\alpha_s^2 e^{\alpha Y}} \exp \left(\frac{1}{\alpha_s^2 e^{\alpha Y}} \right) \Gamma \left(0, \frac{1}{\alpha_s^2 e^{\alpha Y}} \right) \left[4 + \frac{10}{\alpha_s^2 e^{\alpha Y}} + \frac{3}{(\alpha_s^2 e^{\alpha Y})^2} \right] - \left[\frac{7}{\alpha_s^2 e^{\alpha Y}} + \frac{3}{(\alpha_s^2 e^{\alpha Y})^2} \right] \right\} \\ &+ (\alpha_s^2) \left\{ \tilde{f}_1(\alpha_s^2 e^{\alpha Y}) \right\} + (\alpha_s^2 e^{\alpha Y})^2 \left\{ \tilde{f}_2(\alpha_s^2 e^{\alpha Y}) \right\} + \dots , \end{aligned} \quad (16)$$

however, it gets considerably simplified when $\alpha_s^2 e^{\alpha Y}$ becomes large,

$$S(Y) = \frac{1}{\alpha_s^2 e^{\alpha Y}} \exp \left(\frac{1}{\alpha_s^2 e^{\alpha Y}} \right) \Gamma \left(0, \frac{1}{\alpha_s^2 e^{\alpha Y}} \right) \left[1 + 4\alpha_s^2 \alpha Y + \mathcal{O} \left(\frac{1}{\alpha_s^2 e^{\alpha Y}} \right) \right] , \quad (17)$$

where $\Gamma(0, x)$ is the incomplete gamma function. The NLO correction term $4\alpha_s^2 \alpha Y$ inside the brackets with respect to the leading contribution is new.

B. Method II: ω -representation

This method exhibits the pole-structure of the toy model

In this section, we develop another more powerful method, the ω -representation, to solve the toy model.

which bears some resemblance to the pole-structure of the BFKL equation in QCD. The ω -representation is equivalent to the integral representation method in Sec. III A, however, it enables us to go one step further by resumming all the $\alpha_s^2 \alpha Y$ terms in the S -matrix. Therefore, this method allows us to get an expression for the S -matrix which is assumed to be valid up to the rapid-

ity $Y_{c2} = \frac{1}{\alpha_s^4 \alpha}$ where the next-to-next-to-leading order $(\mathcal{O}(\alpha_s^4) \alpha Y)$ becomes of order one.

Let us show how to solve Eq. (2) with the ω -representation method. One starts with the Laplace transform of Eq. (2)

$$\omega n^{(k)}(\omega) - n^{(k)}(t) \Big|_{t=0} = kn^{(k)}(\omega) + k(k-1)n^{(k-1)}(\omega) - k\alpha_s^2 n^{(k+1)}(\omega) , \quad (18)$$

where we have used the definitions $t = \alpha y$ and $n^{(k)}(\omega) = \int_0^\infty dt n^{(k)}(t) e^{-\omega t}$. With the initial condition $n_0^{(1)} \Big|_{y=0} = N$ and $n_0^{(k)} \Big|_{y=0}^{k>1} = 0$, Eq. (18) can be written into a matrix form:

$$\begin{pmatrix} \omega - 1 & \alpha_s^2 & 0 & 0 & 0 \\ -2 & \omega - 2 & 2\alpha_s^2 & 0 & 0 \\ 0 & \dots & \dots & \dots & 0 \\ 0 & 0 & -k(k-1) & \omega - k & k\alpha_s^2 \\ 0 & 0 & 0 & \dots & \dots \end{pmatrix} \cdot \begin{pmatrix} n^{(1)}(\omega) \\ n^{(2)}(\omega) \\ \dots \\ n^{(k)}(\omega) \\ \dots \end{pmatrix} = \begin{pmatrix} N \\ 0 \\ 0 \\ 0 \\ 0 \end{pmatrix} . \quad (19)$$

It is fairly complicated to solve this equation directly because of the infinite dimension it has. Nevertheless, there are two ways to attack this problem. First, we can follow the idea that the α_s^2 is small, which reduces the importance of recombination at the beginning of the evolution. Then we can solve the above linear algebra equation perturbatively which will prove that this approach is completely equivalent to the integral representation method we developed in the previous section. Second, noticing that Eq. (19) has an exact solution at finite dimensions, we can truncate the Eq. (19) to a $k \times k$ linear algebra equation and then take the $k \rightarrow \infty$ limit to get the solution of our infinite dimension matrix.

First, let us turn off the perturbation and only solve the unperturbed matrix to get the corresponding $n_0^{(k)}(\omega)$. One can easily find the solution to be $n_0^{(k)}(\omega) = \frac{N(k-1)!k!}{(\omega-1) \cdot (\omega-2) \cdots (\omega-k)} = \frac{N(k-1)!k!\Gamma(\omega-k)}{\Gamma(\omega)}$. After the inverse Laplace transformation,

$$n_0^{(k)}(\alpha y) = \frac{1}{2\pi i} \int_{s-i\infty}^{s+i\infty} d\omega e^{\omega \alpha y} n_0^{(k)}(\omega), \quad (20)$$

$$= Nk!e^{k\alpha y}(1 - e^{-\alpha y})^{k-1} , \quad (21)$$

the result is exactly the same as what we have obtained in the previous section.

Turning on the perturbation, we find that the first-order correction $\Delta n_1^{(k)}(\omega)$ to $n_0^{(k)}(\omega)$ satisfies the equation:

$$\begin{pmatrix} \omega - 1 & 0 & 0 & 0 & 0 \\ -2 & \omega - 2 & 0 & 0 & 0 \\ 0 & \dots & \dots & 0 & 0 \\ 0 & 0 & -k(k-1) & \omega - k & 0 \\ 0 & 0 & 0 & \dots & \dots \end{pmatrix} \cdot \begin{pmatrix} \Delta n_1^{(1)}(\omega) \\ \Delta n_1^{(2)}(\omega) \\ \dots \\ \Delta n_1^{(k)}(\omega) \\ \dots \end{pmatrix} = \begin{pmatrix} -\alpha_s^2 n_0^{(2)}(\omega) \\ -2\alpha_s^2 n_0^{(3)}(\omega) \\ \dots \\ -k\alpha_s^2 n_0^{(k+1)}(\omega) \\ \dots \end{pmatrix} . \quad (22)$$

The general solution of this equation is too complicated to be written down. However, the strategy of how to get it is straightforward. For example, we can easily obtain $\Delta n_1^{(1)}(\omega) = \frac{-2\alpha_s^2 N}{(\omega-1)^2 \cdot (\omega-2)}$ which corresponds to the one-loop diagram. It yields the same result as given in Eq. (6) after the inverse Laplace transformation. This example

shows that the result for each diagram calculated in the previous section becomes pretty much simplified in the ω -representation. To see this more clearly, one can do the

Laplace transform of Eq. (11) and Eq. (12) which yields

$$\Delta n_m^{(k)}(\omega) = \frac{-k\alpha_s^2}{\omega - k} \Delta n^{(k+1)}(\omega), \quad (23)$$

$$\Delta n_s^{(k)}(\omega) = \frac{k(k-1)}{\omega - k} \Delta n^{(k-1)}(\omega). \quad (24)$$

According to these equations, one can directly write down the contribution for any diagram in this ω -representation

since the merging of $k+1$ -particles to k -particles is nothing but adding a $\frac{1}{\omega-k}$ pole with a prefactor $-k\alpha_s^2$ in ω -complex plane and the splitting of $k-1$ -particles to k -particles is nothing but adding a $\frac{1}{\omega-k}$ pole with a prefactor $k(k-1)$. Although the problem has been simplified a lot in the ω -representation, the exact solution to Eq. (19) is nevertheless unavailable this way.

We get the solution to Eq. (19) as follows: We first truncate the infinite dimension matrix (19) into a finite $k \times k$ matrix, then exactly solve the amputated equation. Let us show the solutions for the first four k -values:

• $k = 1$ case: One obtains $n_{1 \times 1}^{(1)}(\omega) = \frac{N}{\omega-1}$ which transforms to $n_0^{(1)}(\alpha Y) = Ne^{\alpha Y}$.

• $k = 2$ case: One obtains $n_{2 \times 2}^{(1)}(\omega) = \frac{N(\omega-2)}{(\omega-1)(\omega-2)+2\alpha_s^2}$ which transforms to

$$n_1^{(1)}(\alpha Y) = \frac{1-2\alpha_s^2}{1-4\alpha_s^2} Ne^{(1+2\alpha_s^2)\alpha Y} - \frac{2\alpha_s^2}{1-4\alpha_s^2} Ne^{(2-2\alpha_s^2)\alpha Y}. \quad (25)$$

• $k = 3$ case: One obtains $n_{3 \times 3}^{(1)}(\omega) = \frac{N[(\omega-2)(\omega-3)+12\alpha_s^2]}{(\omega-1)(\omega-2)(\omega-3)+2\alpha_s^2(7\omega-9)}$. Then one can set the determinant $(\omega-1)(\omega-2)(\omega-3)+2\alpha_s^2(7\omega-9) = 0$ which yields three solutions. Each of those three solutions stands for three poles $\omega_1 = 1+2\alpha_s^2$, $\omega_2 = 2+10\alpha_s^2$ and $\omega_3 = 3-12\alpha_s^2$, respectively. The inverse Laplace transform changes the integer exponents to non-integer renormalized exponents,

$$n_2^{(1)}(\alpha Y) = \frac{1+3\alpha_s^2}{1+\alpha_s^2} Ne^{(1+2\alpha_s^2)\alpha Y} - \frac{2\alpha_s^2+100\alpha_s^4}{1-14\alpha_s^2} Ne^{(2+10\alpha_s^2)\alpha Y} + \frac{72\alpha_s^4}{1-31\alpha_s^2} Ne^{(3-12\alpha_s^2)\alpha Y}. \quad (26)$$

• $k = 4$ case: One obtains $n_{4 \times 4}^{(1)}(\omega) = \frac{N[(\omega-2)(\omega-3)(\omega-4)+24\alpha_s^2(2\omega-5)]}{(\omega-1)(\omega-2)(\omega-3)(\omega-4)+2\alpha_s^2(72-91\omega+25\omega^2)+72\alpha_s^4}$. The denominator has 4 poles which are $\omega_1 = 1+2\alpha_s^2 + o(\alpha_s^4)$, $\omega_2 = 2+10\alpha_s^2 + o(\alpha_s^4)$, $\omega_3 = 3+24\alpha_s^2 + 1164\alpha_s^4$ and $\omega_4 = 4-36\alpha_s^2 - 1080\alpha_s^4$. Then, the inverse Laplace transform gives

$$\begin{aligned} n_3^{(1)}(\alpha Y) = & N(1+o(\alpha_s^2)) e^{(1+2\alpha_s^2)\alpha Y} - 2!N\alpha_s^2(1+o(\alpha_s^2)) e^{(2+10\alpha_s^2)\alpha Y} \\ & + 3!N\alpha_s^4(1+o(\alpha_s^2)) Ne^{(3+24\alpha_s^2)\alpha Y} - 7344(\alpha_s^6) Ne^{(4-36\alpha_s^2)\alpha Y}. \end{aligned} \quad (27)$$

From the above calculation for $n^{(1)}(\alpha Y)$, one can already see that for an arbitrary k , the first $k-1$ poles are stabilized to the corresponding solutions $\omega_j = j+(3j^2-j)\alpha_s^2 + \mathcal{O}(\alpha_s^4)$ ($1 \leq j \leq k$) with a fixed coefficient $j!N(\alpha_s^2)^{j-1}$ and the last pole is always $\omega_k = k-k(k-1)^2\alpha_s^2 + \mathcal{O}(\alpha_s^4)$ with a wrong coefficient since it misses the recombination from $(k+1)$ particle mode as a result of truncation at the k particle mode. In addition, it is easy to see that the $(3j^2-j)\alpha_s^2$ term is corresponding to the sum of the

NLO contributions $(j+1)j^2\alpha_s^2\alpha Y$ of the leading loop diagrams (e.g. Fig. 1 B) and the leading contributions $(-j(j-1)^2\alpha_s^2\alpha Y)$ of the NLO loop diagrams (Fig. 1 C). On the other hand, the $-k(k-1)^2\alpha_s^2$ term in the last pole only corresponds to the leading order contributions of the NLO loop diagrams (e.g. Fig. 1 C) as a consequence of the truncation at dimension k which rules out the leading loop diagram but allows the NLO loop diagrams at the k particle mode.

The pattern of the exact solution is transparent from the above discussion and the generalization to infinite dimensions follows by simply taking the limit $k \rightarrow \infty$. The exact solution for the S -matrix in infinite dimensions reads

$$S_{exact}(\alpha Y) = \sum_{k=0}^{\infty} (-1)^k (\alpha_s^2)^k k! e^{(k+k(3k-1)\alpha_s^2)\alpha Y + \mathcal{O}(\alpha_s^4)\alpha Y} (1 + \mathcal{O}(\alpha_s^2)). \quad (28)$$

This result agrees with what we have found in the previous section, see Eq. (15), however, it goes a step further since the $k(3k-1)\alpha_s^2\alpha Y$ term is now in the exponent which can be understood as a resummation of all $\alpha_s^2\alpha Y$ terms via exponentiation in Eq. (15).

We notice that the S -matrix is not Borel-summable since $e^{3\alpha_s^2\alpha Y k^2}$ is beyond the Borel-summability according to Nevanlinna's theorem [23]. However, one can generalize the Borel-summation technique and show that the above series still has a finite sum by using analytic continuation. Generally speaking, one can see that the S -matrix is the analytic function of two independent vari-

ables, α_s^2 and αY , when α_s^2 is negative in the α_s^2 complex plane. Since $\alpha_s^2 = 0$ is not a singularity, one can use analytic continuation to define the other half plane when α_s^2 becomes positive. In the following, we provide a generalized Borel-summation method which yields a finite result.

We use a technique together with a subsequent Borel-summation in order to maneuver the divergent series Eq. (28) into a definite and well-defined sum. Let us define $u = \alpha_s^2 e^{(1-\alpha_s^2)\alpha Y}$ and $\gamma = 3\alpha_s^2\alpha Y$, then we obtain

$$S(\alpha Y) = \sum_{k=0}^{\infty} (-1)^k k! u^k e^{\gamma k^2}, \quad (29)$$

$$= \sum_{k=0}^{\infty} (-1)^k \left(\frac{1}{u} \int_0^{\infty} db b^k e^{-\frac{b}{u}} \right) \left(\sqrt{\frac{\gamma}{\pi}} \int_{-\infty}^{+\infty} dx \exp(-\gamma x^2 + 2\gamma x k) \right), \quad (30)$$

$$= \sqrt{\frac{\gamma}{\pi}} \int_{-\infty}^{+\infty} dx \exp(-\gamma x^2) \frac{1}{u} \int_0^{\infty} db \exp\left(-\frac{b}{u}\right) \frac{1}{1+be^{+2\gamma x}}, \quad (31)$$

$$= \sqrt{\frac{\gamma}{\pi}} \int_{-\infty}^{+\infty} dx \exp(-\gamma x^2) \frac{1}{ue^{+2\gamma x}} \exp\left(\frac{1}{ue^{+2\gamma x}}\right) \Gamma\left(0, \frac{1}{ue^{+2\gamma x}}\right). \quad (32)$$

To check the convergence of this integral, one can expand $\Gamma(0, z)$ at $z \rightarrow \infty$ which gives $\Gamma(0, z) \simeq \frac{\exp(-z)}{z} (1 - \frac{1}{z})$, showing that the above integral is definitely finite and well-defined. The x -integration can not be performed analytically. However, one can use the saddle point approximation to evaluate the above x -integral, in which one finds the saddle point $x = -1$, and

$$S(\alpha Y) = \sqrt{\frac{\gamma}{\pi}} \int_{-\infty}^{+\infty} dx \exp(-\gamma x^2 - 2\gamma x) \frac{1}{u} \exp\left(\frac{1}{ue^{+2\gamma x}}\right) \Gamma\left(0, \frac{1}{ue^{+2\gamma x}}\right) \quad (33)$$

$$\approx \frac{1}{\alpha_s^2 e^{(1-4\alpha_s^2)\alpha Y}} \exp\left(\frac{1}{\alpha_s^2 e^{(1-7\alpha_s^2)\alpha Y}}\right) \Gamma\left(0, \frac{1}{\alpha_s^2 e^{(1-7\alpha_s^2)\alpha Y}}\right). \quad (34)$$

A good agreement of this result with the numerical evaluation of Eq. (31) is shown in Fig. (2,3).

Eq. (34) is a fairly exact result in the high-energy limit since it presumably resums all the sub-leading diagrams up to $\alpha_s^2\alpha Y$ level, only neglects $\mathcal{O}(\alpha_s^2)$ (in the prefactor) and $\mathcal{O}(\alpha_s^4\alpha Y)$ (in the exponent) corrections. If we compare this with Eq. (17) of the previous section, we can see that Eq. (17) is an approximate solution which results from Eq. (34) when $\alpha_s^2\alpha Y \ll 1$. The ω -representation is equivalent to the integral representation method in Sec. III A, however, it enables us to go one step further by resumming all the $\alpha_s^2\alpha Y$ terms in the S -matrix. Thus, the S -matrix in Eq. (34) is assumed to be valid up to the rapidity $Y_{c2} = \frac{1}{\alpha_s^2\alpha}$ where the next-to-next-to-leading order ($\mathcal{O}(\alpha_s^4\alpha Y)$) becomes of order one.

C. The Consequences of the NLO Correction

In Mueller's toy model [1], which was inspired by the QCD dipole model [18], the S -matrix for particle-particle scattering in the center-of-mass frame is given by

$$S^{Mueller}(Y) = \sum_{m,n=1}^{\infty} e^{-\alpha_s^2 mn} P_m\left(\frac{\alpha Y}{2}\right) P_n\left(\frac{\alpha Y}{2}\right) \quad (35)$$

where $P_n(Y) = e^{-\alpha Y} (1 - e^{\alpha Y})^{n-1}$ is the probability density of having n particles in the wavefunction of an initial single particle after the evolution up to Y . Expanding the exponential $e^{-\alpha_s^2 mn}$ in Eq. (35) and working up to the NLO, one ends up with a divergent series in the form

$$S^{Mueller}(Y) = \sum_{k=0}^{\infty} (-1)^k \cdot k! (\alpha_s^2 e^{\alpha Y})^k \left[1 - \frac{(k-1)}{e^{\alpha Y/2}} \right] \quad (36)$$

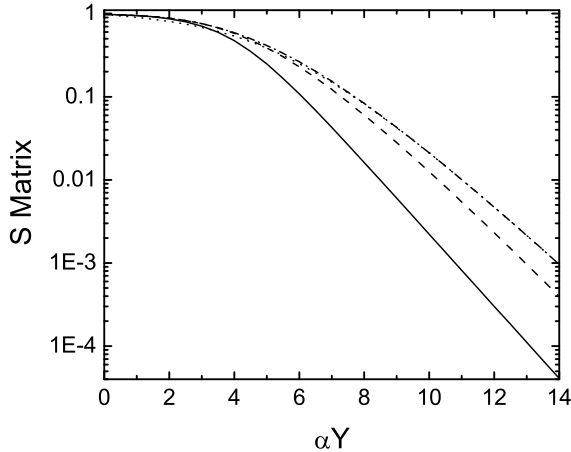


FIG. 2: The S -matrix as a function of αY for $\alpha_s^2 = 0.02$ in logarithmic scale: The solid line represents the solution of the zero-transverse dimensional Kovchegov equation. The dashed line corresponds to the leading order result, the dotted line stands for the saddle point approximation (34) and the dot-dashed line is extracted from the numerical evaluation of Eq. (31).

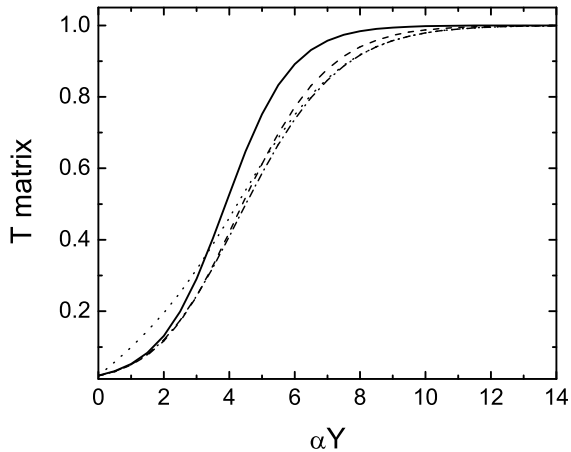


FIG. 3: The T -matrix as a function of αY for $\alpha_s^2 = 0.02$: The solid line represents the solution of the zero-transverse dimensional Kovchegov equation. The dashed line corresponds to the leading order result, the dotted line stands for the saddle point approximation (34) and the dot-dashed line is extracted from the numerical evaluation of Eq. (31).

which after the Borel-summation, for large $\alpha_s^2 e^{\alpha Y}$, becomes

$$S^{Mueller}(Y) = \frac{1}{\alpha_s^2 e^{\alpha Y}} \exp\left(\frac{1}{\alpha_s^2 e^{\alpha Y}}\right) \Gamma\left(0, \frac{1}{\alpha_s^2 e^{\alpha Y}}\right) \times \left[1 + \frac{2}{e^{\alpha Y/2}}\right]. \quad (37)$$

The LO contribution in Eq. (37) is the same as the LO contribution in Eqs. (16,17), however, the NLO contributions are different. Mueller's toy model resums consistently the LO contribution of the LO diagrams (e.g. Fig 1 B), but it does not include the NLO contribution of the LO diagrams (terms including $(k-1)^2 \alpha Y / e^{\alpha Y}$ in Eq. (13)) and also not the NLO loop diagrams (e.g. Fig 1 C).

It was believed that Mueller's toy model (also the QCD dipole model) is correct up to the rapidity $Y_s = \frac{2}{\alpha} \ln\left(\frac{1}{\alpha_s^2}\right)$, at which NLO loop corrections were expected to become nonnegligible which are not included. However, the NLO contribution starts to become comparable to the LO contribution at $Y_c = \frac{1}{\alpha_s^2 \alpha}$, as can be seen from Eq. (17), instead of the rapidity limit $Y_s = \frac{2}{\alpha} \ln\left(\frac{1}{\alpha_s^2}\right)$ that one originally used to believe. Thus, Mueller's result (37) is adequate over a much larger range of rapidity, namely up to $Y_c = \frac{1}{\alpha_s^2 \alpha}$.

Observations made by investigating Mueller's toy model [1] have been shown numerically by Salam [19, 20] to be valid also in the four-dimensional QCD. Presumably our toy model reveals properties of the four-dimensional QCD evolution to some extent. The behavior of our toy model is heuristically indicating that NLO contributions can be neglected in the four-dimensional QCD evolution as long as $Y \ll Y_c$ as well. This belief is strengthened even more by noticing that the NLO correction $\alpha_s^2 \alpha Y$ seem to naturally appear in QCD as well: For the one-loop diagram for instance, the LO contribution in QCD is $(\alpha_s^2)^2 \exp(2\alpha Y)$ which comes from varying the size of the loop from 0 to Y . The NLO contribution $(\alpha_s^2)^2 \alpha Y \exp(\alpha Y)$ comes from changing the location of a fixed zero-size loop from 0 to Y . The NLO contribution is suppressed by the factor $\alpha Y / e^{\alpha Y}$ with respect to the LO contribution, as in the toy model (see Eq. (13)), leading to the general form $\alpha_s^2 \alpha Y$.

Salam has numerically simulated the dipole-dipole scattering [19, 20] based on Mueller's QCD dipole model. He has directly calculated the QCD analog of Eq. (35), instead of following the Borel-summation procedure as outlined below Eq. (35). Salam's numerical calculation corresponds to directly perform the sum in Eq.(35), which gives

$$S^{(Salam)}(Y) = e^{-\alpha Y} \sum_{n=1}^{\infty} \frac{e^{-n/e^{\alpha Y/2}}}{e^{\alpha_s^2 n} - 1 + e^{-\alpha Y/2}}. \quad (38)$$

The competition of $e^{\alpha_s^2 n} - 1$ and $e^{-\alpha Y/2}$ in the denominator leads to two different results for the S -matrix when

$\alpha_s^2 e^{\alpha Y}$ is large

$$S^{(Salam)}(Y) \approx \frac{1}{\alpha_s^2 e^{\alpha Y}} \min \left\{ \ln \left(\alpha_s^2 e^{\alpha Y} \right), \ln \left(\frac{1}{\alpha_s^2} \right) \right\} \quad (39)$$

The transition from first result to the second one occurs at $Y_s = \frac{2}{\alpha} \ln \left(\frac{1}{\alpha_s^2} \right)$ when we evolve the system from low energy to high energy. On the other hand, the Borel summation approach (37) sticks to the first term in above equation, and such transition is absent. We believe that this transition is unphysical while the Borel-summation gives the correct S -matrix and it should be understood as a sign where Salam's numerical calculation breaks down.

An extension of Salam's numerical simulation [19, 20] up to $Y_c = \frac{1}{\alpha_s^2 \alpha}$ in the sense of the Borel-summation technique is also not possible because of the following reason: Salam has found that the S -matrix coming from the QCD dipole model is a multiple Pomeron divergent series (as the series in both toy models) since the ratio of the k to $(k-1)$ -Pomeron exchange amplitude is proportional to k . This prevents any truncation at any arbitrary number k which is needed in order to do the numerical simulation if we work in terms of k -pomeron exchange.

IV. CONCLUSION

We have investigated a stochastic toy model without transverse dimensions (equivalently, a infinite dimension hierarchy of evolution equation) which naturally generates Pomeron loops. We have computed the Pomeron loop diagrams to the NLO using two different methods. We find that the LO calculation yields the same result as what Mueller has shown in Ref. [1]. The study of NLO graphs in this toy model generates the $(\alpha_s^2 \alpha Y)$ corrections.

In the following, we would like to qualitatively discuss about what we can heuristically learn from this toy model for the real QCD in four dimensions, which is:

- Mueller's calculation for dipole-dipole scattering based on the QCD dipole model, which only resums the leading order Pomeron-loop diagrams, seems to be valid up to rapidity $\frac{1}{\alpha \alpha_s^2}$, instead of $\frac{2}{\alpha} \ln \left(\frac{1}{\alpha_s^2} \right)$ as believed. We believe that the NLO correction in four-dimensional QCD would be of order $\alpha_s^2 \alpha Y$ as well (here we define $\alpha = \alpha_P - 1 = \frac{4 \alpha_s N_c}{\pi} \ln 2$ to be the BFKL pomeron intercept). For the one-Pomeron loop diagram for example, the leading order should be of order $(\alpha_s^2)^2 \exp(2\alpha Y)$ which comes from varying the size of the loop from 0 to Y , then the NLO contribution $(\alpha_s^2)^2 \alpha Y \exp(\alpha Y)$ comes from fixing the size of the loop but changing the location of the loop from 0 to Y . Then, we can see that the NLO correction generally takes the form of $\alpha_s^2 \alpha Y$. As a consequence, one can neglect the saturation effect in the wavefunction, and

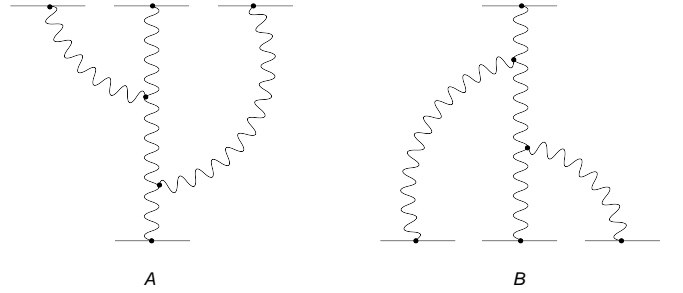


FIG. 4: Graphs for one object scattering with three objects. Curly lines represent BFKL ladders. In graph (A) a single particle evolves through Pomeron splittings and scatters off three particles, while in graph (B) three particles evolve through Pomeron mergings and scatter off a single particle.

just need to calculate the LO diagrams in which all the splittings happen before all the mergings in real QCD. The result should be valid up to the limit $\frac{1}{\alpha \alpha_s^2}$.

- Salam's numerical simulation can not be directly extended up to $\frac{1}{\alpha \alpha_s^2}$ unless a new numerical method is developed to cure pathological behavior of Eq. (35), which intrinsically limits the numerical simulation to $Y_s \leq \frac{2}{\alpha} \ln \left(\frac{1}{\alpha_s^2} \right)$.

Acknowledgments

We would like to thank Alfred Mueller for numerous stimulating and insightful discussions. We are also grateful to Stephane Munier for many useful remarks and comments. A. Sh. acknowledges financial support by the Deutsche Forschungsgemeinschaft under contract Sh 92/2-1.

APPENDIX A: THE EQUIVALENCE OF SPLITTING AND RECOMBINATION

In this part, we show that Eq. (2) gives Lorentz invariant results. To show this, let us start with a single particle, then split it to three particles which yields $n_0^{(3)}(y) = N 3! e^{3\alpha y} (1 - e^{-\alpha y})^2$ according to Eq. (4). Following Kovchegov [24], the scattering amplitude is

$$A(\alpha Y) = \sum_{k=1}^{\infty} \frac{(-1)^{k+1}}{k!} n_0^{(k)}(Y) T^{(k)}(0). \quad (A1)$$

in which $T^{(k)}(0) = (\alpha_s^2)^k$ and the $\frac{1}{k!}$ can be understood as the fact that those k -particles in the target are the same. Therefore, it is very easy to see that $A_s(\alpha Y) = N (\alpha_s^2 e^{\alpha Y})^3 e^{3\alpha y} (1 - e^{-\alpha y})^2$ which corresponds to the diagram shown in Fig. 4 A.

On the other hand, we can put the evolution into the target, let them merge into one object before scattering with the projectile (Fig. 4 B). This means that one starts with an initial condition $n_0^{(3)}\Big|_{y=0} = N_3$ and $n_0^{(k)}\Big|_{y=0}^{k \neq 3} = 0$ in solving the Eq. (2). After merging twice from $n_0^{(3)}(y) = N_3 e^{3\alpha y}$, one obtains $\Delta n^{(1)} = N_3 \left(\frac{\beta}{\alpha}\right)^2 e^{3\alpha y} (1 - e^{-\alpha y})^2$. Finally, it is straight forward

to see that $A_m(\alpha Y) = N_3 (\alpha_s^2 e^{\alpha y})^3 e^{3\alpha y} (1 - e^{-\alpha y})^2$ after setting $\frac{\beta}{\alpha} = \alpha_s^2$. Presumably, $A_s(\alpha Y)$ should be same as $A_m(\alpha Y)$ since they actually describe the same process, and they are indeed the same once we set $N = N_3$.

Moreover, it is tempting to replace the target by a large nucleus with A nucleons inside it. Then, we need to define $T^{(k)}(0) = \left(A^{\frac{1}{3}}\alpha_s^2\right)^k$, and indeed one can see that $A_s(\alpha Y) = A_m(\alpha Y)$ as long as we set $N_3 = N \left(A^{\frac{1}{3}}\right)^3$.

APPENDIX B: SOLUTION TO A SLIGHTLY DIFFERENT STOCHASTIC DIFFERENTIAL EQUATION

We notice that there has been a lot of theoretical discussion and numerical simulation on a slightly different stochastic differential equation which has a noise term $\sqrt{2(\alpha\tilde{n} - \beta\tilde{n}^2)}\nu(y)$, namely the stochastic Fisher-Kolmogorov-Petrovsky-Piscounov(sFKPP) equation. For completeness, we provide the solution to this equation by using the ω -representation we developed above. The dynamics of this equation is given by two random processes: by an increase dY in rapidity, a particle can split into two particles with some rate α ($A \xrightarrow{\alpha} A + A$) or two particles can merge into one with a rate 2β ($A + A \xrightarrow{2\beta} A$). From the equation,

$$\frac{d\tilde{n}}{dy} = \alpha\tilde{n} - \beta\tilde{n}^2 + \sqrt{2(\alpha\tilde{n} - \beta\tilde{n}^2)}\nu(y), \quad (\text{B1})$$

one can get

$$\frac{dn^{(k)}}{dy} = (k\alpha - k(k-1)\beta) n^{(k)} + k(k-1)\alpha n^{(k-1)} - k\beta n^{(k+1)}. \quad (\text{B2})$$

Similarly, one can write Eq. (B2) into a matrix in the ω -representation, then get the similar S -matrix of the scattering between two dipoles.

$$S(\alpha Y) = \sum_{k=0}^{\infty} (-1)^k (\alpha_s^2)^k k! e^{(k+2k^2\alpha_s^2)\alpha Y + o(\alpha_s^4)\alpha Y} (1 + o(\alpha_s^2)), \quad (B3)$$

$$= \sqrt{\frac{\delta}{\pi}} \int_{-\infty}^{+\infty} dx \exp(-\delta x^2) \frac{1}{v e^{+2\delta x}} \exp\left(\frac{1}{v e^{+2\delta x}}\right) \Gamma\left(0, \frac{1}{v e^{+2\delta x}}\right) \quad (B4)$$

$$\approx \frac{1}{\alpha_s^2 e^{(1-2\alpha_s^2)\alpha Y}} \exp\left(\frac{1}{\alpha_s^2 e^{(1-4\alpha_s^2)\alpha Y}}\right) \Gamma\left(0, \frac{1}{\alpha_s^2 e^{(1-4\alpha_s^2)\alpha Y}}\right), \quad (B5)$$

where $\delta = 2\alpha_s^2 \alpha Y$ and $v = \alpha_s^2 e^{\alpha Y}$. The difference of between this result and the one in Eq. (34) is at the NLO correction, however, one can see that Eq. (1) has a more transparent physical meaning in QCD since it contains the projectile-target duality and one can easily relate it to the zero transverse dimension reggeon theory.

- [1] A. H. Mueller, Nucl. Phys. B **437** (1995) 107.
- [2] A. H. Mueller and A. I. Shoshi, Nucl. Phys. B **692** (2004) 175.
- [3] E. Iancu, A. H. Mueller and S. Munier, Phys. Lett. B **606** (2005) 342.
- [4] S. Munier and R. Peschanski, Phys. Rev. Lett. **91** (2003) 232001; Phys. Rev. D **69** (2004) 034008.
- [5] E. Iancu and D. N. Triantafyllopoulos, Nucl. Phys. A **756** (2005) 419.
- [6] I. Balitsky, Nucl. Phys. B **463** (1996) 99; Phys. Rev. Lett. **81** (1998) 2024; Phys. Lett. B **518** (2001) 235.
- [7] J. Jalilian-Marian, A. Kovner, A. Leonidov and H. Weigert, Nucl. Phys. B **504** (1997) 415; Phys. Rev. D **59** (1999) 014014;
E. Iancu, A. Leonidov and L. D. McLerran, Phys. Lett. B **510** (2001) 133; Nucl. Phys. A **692** (2001) 583;
H. Weigert, Nucl. Phys. A **703** (2002) 823.
- [8] A. H. Mueller, A. I. Shoshi and S. M. H. Wong, Nucl.

Phys. B **715** (2005) 440.

[9] E. Iancu and D. N. Triantafyllopoulos, Phys. Lett. B **610** (2005) 253.

[10] A. Kovner and M. Lublinsky, Phys. Rev. D **71** (2005) 085004.

[11] Y. Hatta, E. Iancu, L. McLerran, A. Stasto and D. N. Triantafyllopoulos, arXiv:hep-ph/0504182.

[12] A. Kovner and M. Lublinsky, Phys. Rev. Lett. **94** (2005) 181603; JHEP **0503** (2005) 001; Phys. Rev. D **72** (2005) 074023; “More remarks on high energy evolution,” arXiv:hep-ph/0510047.

[13] J. P. Blaizot, E. Iancu, K. Itakura and D. N. Triantafyllopoulos, Phys. Lett. B **615** (2005) 221.
Y. Hatta, E. Iancu, L. McLerran and A. Stasto, Nucl. Phys. A **762** (2005) 272.
E. Iancu, G. Soyez and D. N. Triantafyllopoulos, “On the probabilistic interpretation of the evolution equations with Pomeron arXiv:hep-ph/0510094.

[14] C. Marquet, A. H. Mueller, A. I. Shoshi and S. M. H. Wong, Nucl. Phys. A **762** (2005) 252.

[15] E. Levin and M. Lublinsky, “Towards a symmetric approach to high energy evolution: Generating functional with Pomeron loops,” arXiv:hep-ph/0501173.

[16] R. Enberg, K. Golec-Biernat and S. Munier, Phys. Rev. D **72** (2005) 074021.

[17] G. Soyez, Phys. Rev. D **72** (2005) 016007.

[18] A. H. Mueller, Nucl. Phys. B **415** (1994) 373; Nucl. Phys. B **425** (1994) 471.

[19] G. P. Salam, Nucl. Phys. B **461** (1996) 512;

[20] G. P. Salam, Nucl. Phys. B **449** (1995) 589.

[21] Y. V. Kovchegov, Phys. Rev. D **72** (2005) 094009.

[22] A. H. Mueller and G. P. Salam, Nucl. Phys. B **475**, 293 (1996).

[23] G.H. Hardy, Divergent Series(Oxford University, Oxford, 1963).

[24] Y. V. Kovchegov, Phys. Rev. D **60** (1999) 034008.